Cell Biochem Biophys
DOI 10.1007/s12013-012-9467-6

ORIGINAL PAPER

Differential Effects of G- and F-Actin on the Plasma Membrane Calcium Pump Activity

Laura Vanagas · María Candelaria de La Fuente · Marianela Dalghi · Mariela Ferreira-Gomes · Rolando C. Rossi · Emanuel E. Strehler · Irene C. Mangialavori · Juan P. F. C. Rossi

Abstract We have previously shown that plasma membrane calcium ATPase (PMCA) pump activity is affected by the membrane protein concentration (Vanagas et al., Biochim Biophys Acta 1768:1641–1644, 2007). The results of this study provided evidence for the involvement of the actin cytoskeleton. In this study, we explored the relationship between the polymerization state of actin and its effects on purified PMCA activity. Our results show that PMCA associates with the actin cytoskeleton and this interaction causes a modulation of the catalytic activity involving the phosphorylated intermediate of the pump. The state of actin polymerization determines whether it acts as an activator or an inhibitor of the pump: G-actin and/or short oligomers activate the pump, while F-actin inhibits it. The effects of actin on PMCA are the consequence of direct interaction as demonstrated by immunoblotting and cosedimentation experiments. Taken together, these findings suggest that interactions with actin play a dynamic role in the regulation of PMCA-mediated Ca^{2+} extrusion through the membrane. Our results provide further evidence of the activation–inhibition phenomenon as a property of many cytoskeleton-associated membrane proteins where the cytoskeleton is no longer restricted to a mechanical function but is dynamically involved in modulating the activity of integral proteins with which it interacts.

Keywords PMCA · Cytoskeleton · Actin · Regulation

Abbreviations

DMSO	Dimethyl sulfoxide
EGTA	Ethylene glycol tetraacetic acid
IOVs	Inside-out vesicles
MESG	2-Amino-6-mercapto-7-methylpurine riboside
PMCA	Plasma membrane calcium ATPase
Tris	Tris(hydroxymethyl) aminomethane
$C_{12}E_{10}$	Polyoxyethylene glycol monoether with C12 alkyl chain and 10 polyoxyethylene units in the headgroup

Introduction

Cytoskeleton–membrane interactions go far beyond simple structural or mechanical linkages between the cytoskeleton and the plasma membranes and are now recognized as dynamic interactions that include newly recognized functions involving signal transduction pathways. Results from diverse studies, e.g., on signal transduction, membrane trafficking, and ion channel function suggest that the cytoskeleton may play a key role not only in the stabilization and delivery but also in activation of the membrane proteins mediating ion transport events (for references see [2]).

Cells can rapidly and reversibly alter solute transport rates by changing the kinetics of transport proteins. At least two molecular mechanisms may be involved in this process: (i) regulation of the transporter kinetics itself such as by phosphorylation of the transporter (i.e., affecting the

Laura Vanagas and María Candelaria de La Fuente are contributed equally to this work.

L. Vanagas · M. C. de La Fuente · M. Dalghi · M. Ferreira-Gomes · R. C. Rossi · I. C. Mangialavori (✉) · J. P. F. C. Rossi
IQUIFIB, Facultad de Farmacia y Bioquímica, Universidad de Buenos Aires, Junín 956 (1113), Buenos Aires, Argentina
e-mail: icmangialavori@yahoo.com.ar

E. E. Strehler
Department of Biochemistry and Molecular Biology, Mayo Clinic College of Medicine, Rochester, MN 55905, USA

Published online: 15 November 2012

turnover rate of the individual transporter) or alternatively (ii) by altering the number of transport proteins per unit area of the plasma membrane. These two mechanisms are not mutually exclusive, and both can be regulated by the actin cytoskeleton [2]. On the other hand, the controlled polymerization and degradation of actin and tubulin is crucial for the mobility and shape of eukaryotic cells. The movement of eukaryotic cells is the result of the coordinated action of the formation of extensions, adhesions, and retractions of the membrane, where the actin network and the interactions between the cytoskeleton and molecular motors play a key role. Changes in ion transport require spatially and temporally coordinated changes in cell morphology and cell motility, and these changes can be brought about by changes in actin dynamics [2].

One molecule of ATP is hydrolyzed during each assembly and disassembly cycle of an actin monomer and the hydrolysis occurs within the polymer. Thus, ATP-bound G-actin monomers assemble to yield a filament consisting of ATP-F-actin in the fast growing end and ADP-F-actin in the opposite end; finally, ADP-monomers are released at the end of the cycle [3]. Nucleotide hydrolysis is not necessary for assembly per se; rather, it provides a conformational switch that drives the cycle of assembly and disassembly. ATP is required to maintain stable actin filaments, and its hydrolysis produces a change in the state of monomers within the filament making it unstable and prone to disassemble. The lifetime of a filament is then determined by how quickly the switch operates [3].

Changes in the cortical cytoskeleton can alter cell morphology drastically, and the proteins associated with actin regulate such changes. For example, Bertorello et al. [4] showed that actin increases Na^+,K^+-ATPase activity by recruiting α-subunits into the plasma membrane from an intracellular compartment in a Na^+-independent manner. A functional role of actin on the pump activity is suggested by studies where addition of actin was associated with an increase in the affinity of the pump for Na^+ but not for other enzymatic substrates [5]. It has been observed that purified Na^+,K^+-ATPase pump associates with actin and this interaction probably involves the α-subunit of the pump which contains a putative actin-binding domain [5].

Recent studies from our laboratory [1] have shown that the specific activity of the Ca^{2+}-ATPase of erythrocyte membranes increased steeply up to 1.5–5 times when the membrane protein concentration decreased from 50 to 1 μg/ml; however, dilution of the protein did not modify the affinities for activation by ATP, Ca^{2+}, or Ca^{2+}-calmodulin. These phenomena were affected by Cytochalasin D, leading us to propose that the concentration-dependent behavior of the PMCA activity was due to interactions with cytoskeletal proteins, in particular actin.

In this study, we explored the relationship between the polymerization state of actin and its effects on purified PMCA activity. Our results show that PMCA associates with the actin cytoskeleton and this interaction causes a modulation on the catalytic activity of the pump. The state of actin polymerization appears to be crucial as G-actin and/or short oligomers activate the pump, while F-actin inhibits it.

These findings provide further support for the notion that the cytoskeleton is not restricted to a merely mechanical function but is dynamically involved in modulating the activity of integral membrane proteins such as the PMCA and Na^+,K^+-ATPase with which it interacts.

Experimental Procedures

Reagents

All chemicals used in this study were of analytical grade and purchased from Sigma Chemical Co. (USA). Recently drawn human blood for the isolation of PMCA was obtained from the Hematology Section of the Hospital de Clínicas General San Martín (Argentina) and from Fundosol Foundation (Argentina).

Isolation of Membranes from Human Erythrocytes

Calmodulin-depleted erythrocyte membranes were prepared according to González Flecha et al. [6]. The membranes were stored in liquid nitrogen until use.

Inside-Out Vesicles (IOVs)

Sealed IOVs were prepared according to Steck et al. [7]. The percentage of IOVs was determined by the method described by Ellman et al. [8], which uses the acetyl cholinesterase activity of the membranes in the presence or absence of detergent (Triton X-100) to open the vesicles.

Purification of PMCA from Human Erythrocytes

PMCA was isolated by calmodulin-affinity chromatography as described elsewhere [9]. Purified PMCA was assayed for protein concentration and homogeneity by SDS-PAGE (350–800 nM; single band at M_r 134,000) and stored in liquid nitrogen until use. PMCA was kept in a buffer containing 20 % (w/v) glycerol, 0.005 % $C_{12}E_{10}$, 120 mM KCl, 1 mM $MgCl_2$, 10 mM MOPS-K (pH 7.4 at 4 °C), 2 mM ethylene glycol tetraacetic acid (EGTA), and 2 mM dithiothreitol (DTT).

Purification of Actin

Actin was extracted from acetone powder of rabbit back leg muscle at 0 °C according to Pardee and Spudich [10]. Protein concentration was determined by measuring the absorbance at 290 nm using an extinction coefficient of 0.63 $(mg/ml)^{-1}$ cm^{-1}. SDS-PAGE was performed to assess the purity of the preparation (typically ≈98 %). Purified monomeric actin was stored frozen at −80 °C after freezing in liquid nitrogen at high concentrations (≥5 mg ml^{-1}) in small volume (≤100 µl). Under this storage condition, the sample is stable for 6 months [11]. At the time of use, frozen samples were thawed rapidly at 37 °C and clarified. Clarification consists of 20× dilution of the sample in fresh Buffer G (2 mM Tris–HCl, 0.2 mM Na_2ATP, 0.5 mM dithiothreitol, 0.2 mM $CaCl_2$, 0.005 % azide, pH 8.0 at 25 °C), leaving the preparation at 4 °C for 1 h to depolymerize actin oligomers that may have formed during the freeze–thaw steps followed by centrifugation at 14,000 rpm at 4 °C for 30 min to remove residual nucleating centers. When needed, actin was polymerized and converted to F-actin by adding 120 mM KCl, 2 mM ATP, and 3.75 mM $MgCl_2$. The actin concentration value always refers to the total number of G-actin monomers although it is F-actin, and not to the number of the polymers.

Actin Polymerization Assay

Pyrene-actin (Cytoskeleton, Inc.) was diluted from stock solution (20 mg/ml) to a final concentration equal to the concentration used for the non-labeled actin and clarified as described above. Pyrene-actin in the supernatant was added to non-labeled actin in order to obtain 6 % of label. Actin polymerization was monitored by registering the change in the fluorescence signal in a thermostated spectrofluorimeter Jasco FP-6500 using a quartz cuvette of 3 × 3 mm. The excitation and emission wavelengths were 365 and 407 nm, respectively, with a bandwidth of 3 and 10 nm [12]. The polymerization reaction was initiated by the addition of a 10× reaction medium stock solution to obtain the same final composition used for Ca^{2+}-ATPase experiments. To avoid bleaching the fluorophore, the sample was exposed to the lamp intermittently, only during recording periods.

Measurement of Ca^{2+}-ATPase Activity

ATPase activity was measured at 25 °C by following the release of inorganic phosphate from ATP by the method of Webb [13] or Fiske and Subbarow [14]. The incubation medium was 1.5 nM PMCA, 30 mM MOPS, 120 mM KCl, 3.75 mM $MgCl_2$, 120 µM $C_{12}E_{10}$, 40 µM soybean phospholipids, 1 mM EGTA, and enough $CaCl_2$ to obtain the concentration of 100 µM $[Ca^{2+}]_{free}$. In experiments where actin polymerization needed to be slowed down, we modified the KCl and $MgCl_2$ concentration to 40 and 0.8 mM, respectively. When the activity was measured as a function of F-actin concentration, G-actin was incubated in the reaction medium during 60 min before the reaction. This time should be sufficient to allow actin to polymerize. The ATPase reaction was started by the addition of 2 mM ATP in all cases.

Gel Electrophoresis

SDS gel electrophoresis was carried out according to the Tris/tricine method [15]. After electrophoresis, the gels were stained with Coomassie Brilliant Blue R.

Determination of Protein Concentration in Membrane and IOVs Preparations

The total protein concentration in membrane preparations was estimated by the method described by Lündahl [16] and by the method of Peterson [17]. Actin present in membrane preparations was identified by immunoblotting (see above) and its concentration was quantified by SDS-PAGE using BSA as standard, as described previously [18].

Determination of Phosphorylated Intermediates

The phosphorylated intermediates (EP) were measured as the amount of acid-stable ^{32}P incorporated in the enzyme (7 nM), according to the method described by Echarte et al. [19]. The phosphorylation was measured at 4 °C in a medium containing 30 mM Tris–HCl (pH 7.4 a 4 °C), 120 mM KCl, 3.75 mM $MgCl_2$, 120 µM $C_{12}E_{10}$, 40 µM soybean phospholipids, 1 mM EGTA, 30 µM [γ-^{32}P]ATP, and enough $CaCl_2$ to obtain 100 µM $[Ca^{2+}]_{free}$. The reaction was started by the addition of [γ-^{32}P]ATP under vigorous stirring and, after 1 min, it was stopped with an ice-cold solution of TCA (10 %, w/v, final concentration). The tubes were centrifuged at 7,000 rpm for 3.5 min at 4 °C. The samples were then washed once with 7 % TCA, 150 mM H_3PO_4, and once with double distilled water and processed for SDS-PAGE. For this purpose, the pellets were dissolved in a medium containing 150 mM Tris–HCl (pH 6.5 at 14 °C), 5 % SDS, 5 % DTT, 10 % glycerol, and bromophenol blue (sample buffer). Electrophoresis was performed at pH 6.3 (14 °C) in a 7.5 % polyacrylamide gel. The reservoir buffer was 0.1 M sodium phosphate, pH 6.3, with 0.1 % SDS. Migration of the sample components took place at 14 °C, with a current of 60 mA until the tracking dye reached a distance of about 10 cm from the top of the gel. Gels were stained, dried, and exposed to a Storage Phospho Screen from Molecular Dynamics (Amersham Pharmacia Biotech). Unsaturated

autoradiograms and stained gels were scanned with an HP Scanjet G2410 scanner. Analysis of the images was performed with GelPro Analyser. EP quantification was achieved as described in Echarte et al. [19].

Immunoblotting

Binding of PMCA to actin was examined by immunoblotting as described previously by Cantiello [5]. Aliquots of purified PMCA and BSA negative control were spotted on activated membranes of nitrocellulose and the membranes were incubated at least 2 h in PBS with 5 % fat-free milk to block cross-reactive proteins. The membranes were then incubated at 4 °C during 2 h on a rocking table in the presence or absence of 5 μM G-actin (in the presence of Buffer G, see above) or F-actin (in the presence of 120 mM KCl and 3.75 mM $MgCl_2$). The membranes were washed six times with a cold solution of PBS-Tween 20 and then incubated for 1 h with the corresponding primary antibodies. A rabbit polyclonal anti-actin antibody from Sigma and the mouse monoclonal anti-PMCA antibody 5F10 were used to detect actin and the PMCA, respectively. The primary antibodies were detected with affinity-purified biotinylated goat anti-rabbit or donkey anti-mouse IgG after incubating for 30 min with streptavidin (BioRad). Blots were developed with a solution of 10 mg of 3,3′-diaminobenzidine in 20 ml of PBS with 10 μl $NiCl_2$ 10 % and 15 μl of H_2O_2 (30 % v/v). Controls for non-specific binding of the anti-actin antibody were performed by incubating the nitrocellulose membrane with PMCA in absence of actin (G- and F-actin). Conversely, PMCA was also incubated in the absence of actin and detected with 5F10.

Actin Cosedimentation

Two different approaches were used in these experiments. The first was an actin-binding spin-down assay kit (Cytoskeleton Cat. BK013). The actin-binding protein spin-down assay kit provides F-actin plus positive (α-actinin) and negative (Bovine Serum Albumin, BSA) binding control protein. Actin binding occurs when there is an affinity for any site of actin. F-actin binding can be measured using a spin-down method. The second procedure was that described by Srivastava and Barber [20]. This assay is extensively used to determine the specific interaction of protein with F-actin and estimate apparent binding affinities. In both cases, the purified and solubilized micelles of PMCA were brought into contact with clarified actin and incubated under conditions which promote the polymerization for 40 min. The samples were ultracentrifuged for 20 min at 100,000×*g*. The proteins present in the supernatants were precipitated with 10 % TCA and, as the pellet, seeded in a SDS-PAGE.

Preparation of [^{125}I]TID-PC/16

TTD-PC/16 (tin precursor) was a kind gift of Dr. J. Brunner (ETHZentrum, Zurich, Switzerland). [^{125}I]TID-PC/16 was prepared by radioiodination of its tin precursor according to Weber and Brunner [21].

Labeling Procedure

Photolabeling assay was carried out as described by Mangialavori et al. [22, 23]. A dried film of the photoactivatable reagent was suspended in PC/$C_{12}E_{10}$ mixed micelles containing 7 nM of PMCA. The samples were incubated for 10 min at 25 °C—except for F-actin condition where incubation was for 60 min–in the presence of 1 mM EGTA (EGTA condition); 100 μM Ca^{2+}_{free} (Ca^{2+} condition); 100 μM Ca^{2+}_{free} and 200 nM calmodulin (CaM condition); 100 μM Ca^{2+}_{free} and 5 μM G-actin in buffer G (G-actin condition) or; 100 μM Ca^{2+}_{free} and 5 μM G-actin subjected to polymerizing condition (F-actin condition). Before, the samples being irradiated for 10 min with light from a filtered UV source ($\lambda = 360$ nm).

Radioactivity and Protein Determination

Electrophoresis was performed according to the Tris–tricine SDS-PAGE method [15]. Polypeptides were stained with Coomassie Blue R, the isolated bands were excised from the gel, and the incorporation of radioactivity was directly measured on a gamma counter. Specific incorporation was calculated as the ratio between measured radioactivity and amount of protein determined for each band.

Data Analysis

Equations were fitted to the results by nonlinear regression based on the Gauss–Newton algorithm using commercial programs (Excel and Sigma-Plot for Windows, the latter being able to provide not only the best fitting values of the parameters but also their standard errors).

Results

Ca^{2+}-ATPase Specific Activity as a Function of Membrane Protein Concentration

The dependence of PMCA Ca^{2+}-ATPase activity on total membrane protein concentration was studied, as shown in Fig. 1, in isolated membranes (panel A) and in IOVs (panel B) obtained from human erythrocytes. As described previously by Vanagas et al. [1], in membranes, the specific

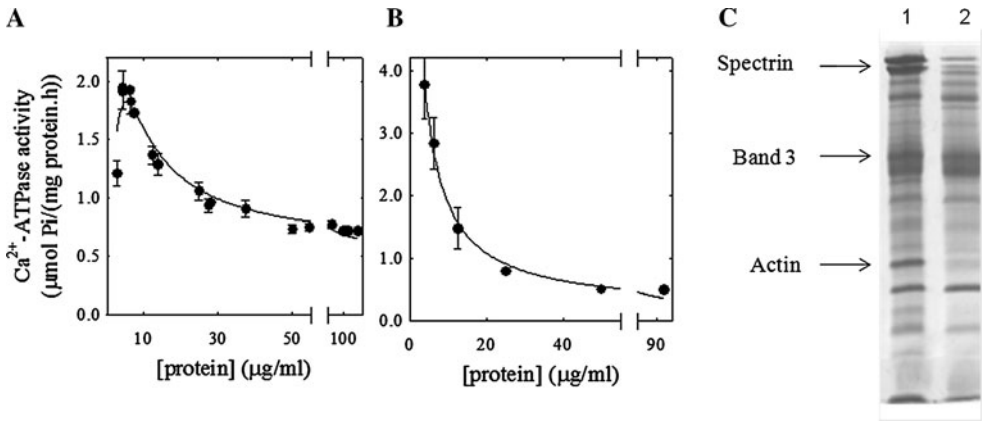

Fig. 1 Ca^{2+}-dependent ATPase activity as a function of membrane protein concentration. ATPase activity was measured as described in materials and methods using erythrocyte membranes (**a**) and IOVs (**b**). The data show the mean ± SD of three to seven independent experiments performed in triplicate. Ca^{2+} concentration was 100 µM. **c** SDS-PAGE of membranes (*lane 1*) and IOVs (*lane 2*). The *arrows* indicate the positions of spectrin, Band 3, and actin. The actin concentration in both preparations was estimated simultaneously by assaying different amounts of bovine serum albumin (not shown). Actin bands were identified by a specific antibody (not shown)

activity first rises at low membrane protein concentration, reaches a maximum and then decreases about 2.8-fold to a value close to 0.7 µmol Pi/(mg protein per h). In contrast, results in Fig. 1b show a continuous decrease in the Ca^{2+}-ATPase activity of about eightfold to a value of around 0.5 µmol Pi/(mg protein/h).

As the SDS-PAGE pattern of erythrocyte membranes has been well established [24], it is possible to identify and quantify the cortical cytoskeleton proteins present in a particular preparation by comparing their electrophoretic mobility. This allows us to relate the level of the increase in the specific activity of PMCA with the amount of actin, or any other cytoskeletal protein, remaining in the preparation. Figure 1c shows that IOVs contain significantly reduced amounts of cytoskeletal proteins (actin, spectrin) compared to isolated membranes. While integral proteins like band 3 did not differ significantly between the two preparations, actin concentration in erythrocyte membranes and IOVs was 1.46 and 0.27 µM, respectively. PMCA concentration corresponds to 0.1 % of total membrane proteins, whereby it cannot be quantified from SDS-PAGE. However, calculations based on the relative value of 0.1 %, yield a PMCA concentration of around 0.1 nM in these preparations.

It is important to note that within the same preparation, the activity increases as total protein concentration (and thus also actin concentration) decreases. One possible explanation for this effect is that actin depolymerization causes PMCA activation as depolymerization is known to occur from actin filaments by dilution. This phenomenon has been studied by Purich and co-workers [25, 26] who have developed a kinetic model for predicting the shape of depolymerization curves after dilution from initial polymer length distributions.

Effect of Actin on Ca^{2+}-ATPase Specific Activity

To further explore whether actin depolymerization was responsible for the Ca^{2+}-ATPase activation, we studied the effect of purified actin on isolated and purified PMCA from erythrocyte membranes. In this case, the Ca^{2+}-ATPase activity was measured continuously by monitoring the release of inorganic phosphate from ATP using the method described by Webb [13]. Figure 2a shows the results of a typical experiment. The control experiment (*gray trace*) was carried out in the presence of 5 µM bovine serum albumin, a protein known to have no effect on PMCA activity. It shows a linear increase in phosphate concentration ($A_{420\ nm}$). From the slope of the plot (Fig. 2b, *gray trace*), we calculated the specific activity which was considered the basal activity of the pump (absence of actin) and was found to be 13.8 ± 0.1 µmol Pi mg^{-1} min^{-1}. When the reaction was initiated in the presence of 5 µM G-actin (Fig. 2a, *black trace*), the experimental data are well described by an exponential plus a linear function (Eq. 1).

$$y = \frac{(a-c)}{k}(1 - e^{-kt}) + ct, \quad (1)$$

where k corresponds to an apparent rate coefficient governing the change in activity, a represents the maximal, initial activity of the pump, and c is the activity that remains after the exponential burst in absorbance has reached its maximum (linear component).

Actin is itself an ATPase, which consumes ATP. The progressive decline in activity observed at later times was not due to substrate depletion. In each experiment, we included a control where actin was incubated in the same reaction medium but with absence of PMCA. The amount

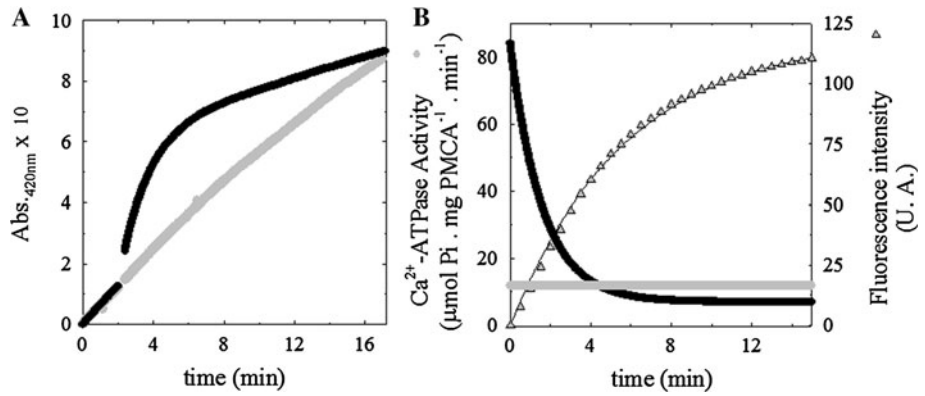

Fig. 2 Effect of actin on purified PMCA activity: **a** typical experiment where Pi released by PMCA was determined by continuously monitoring the absorbance at 420 nm. The reaction was initiated in the presence of 5 µM G-actin (*black trace*), or the same amount of BSA as a control (*gray trace*). **b** Ca^{2+}-ATPase activity was obtained as described in Results and is shown as *black* and *gray* traces, respectively. Note that only shown from time when G-actin was added. These are compared with the polymerization state of actin as determined by monitoring the pyrene-actin fluorescence in the same condition (*triangles*). Mean ± SEM of five to six independent experiments

of Pi released in these condition was less than 5 % of that released in the presence of PMCA (data not shown), discarding the possibility that the decrease in activity was due to the depletion of the substrate.

The time derivative of Eq. 1 yields Eq. 2 that describes how the velocity of the pump changes in these conditions (Fig. 2b, *black trace*):

$$y' = ae^{-kt} + c \tag{2}$$

The best fitting values for the parameters in Eqs. 1 and 2 were $k = 0.6 \pm 0.1$ min^{-1}, $c = 6.9 \pm 0.3$ µmol mg^{-1} min^{-1}, and $a = 77.0 \pm 2.3$ µmol mg^{-1} min^{-1}.

From a comparison in Fig. 2b of the initial stages of the reaction progression in the absence or presence of actin, we can observe that the velocity of the pump in the presence of actin reaches a value that is up to six- to sevenfold than that of the control activity, thus indicating a positive modulatory effect on PMCA activity. Importantly, the degree of PMCA activation varies with time, suggesting that this effect depends on the degree of actin polymerization, as the reaction medium strongly favors actin assembly. This result further supports the evidence that suggests actin depolymerization as the cause of the dilution effect.

In order to correlate both phenomena—the degree of PMCA activation and the state of actin polymerization—we followed the polymerization process under the same experimental conditions as those used for Ca^{2+}-ATPase activity assays, using pyrene labeled actin. The fluorescence of monomeric pyrene-actin is enhanced during its polymerization into filaments, thus constituting an ideal tool for continuous monitoring of actin filament formation [12]. Figure 2b shows that the fluorescence intensity of pyrene-actin (*gray triangles*) increases in time as actin begins to polymerize in the reaction media up to a moment when the fluorescence signal approaches a constant value, indicating that most actin is now in the filamentous form (F-actin). Nonlinear fitting of an increasing exponential function of time to the fluorescence results yielded a value of $k = 0.172 \pm 0.004$ min^{-1}. From these results, it appears that the maximum activation of PMCA Ca^{2+}-ATPase activity corresponds to the first polymerization stages of actin where most actin is thought to be in its monomeric or short oligomer form. Then, as actin polymerization proceeds, PMCA activity progressively decreases. Four minutes after initiation of the reaction, the Ca^{2+}-ATPase activity is similar to that of the control. Finally, when actin progresses toward the filamentous form, Ca^{2+}-ATPase activity decreases to a constant value of about 50 % of the control.

These results lead to two main conclusions: (1) actin itself, without the need of any other protein, can exert an effect on PMCA catalytic activity and (2) its modulatory behavior depends on its polymerization state: while G-actin and/or short oligomers cause an activation of PMCA activity, F-actin has an inhibitory effect although the pump activity is not completely abolished.

Effect of F-Actin Concentration on PMCA Ca^{2+}-ATPase Activity

Different G-actin concentrations were incubated in polymerizing conditions during 1 h in the final activity reaction medium (Fig. 3). In this condition, actin is in the filamentous form (F-actin). The reaction was initiated by addition of ATP as described in "Experimental Procedures" section.

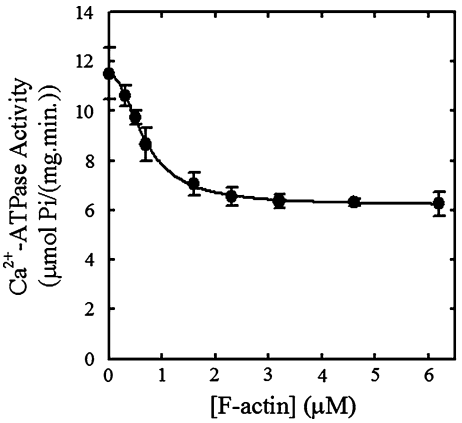

Fig. 3 Effect of F-actin on purified PMCA activity. Different G-actin concentrations were subjected to polymerizing condition in activity reaction medium during 60 min (F-actin). The *black trace* represents the fit of Eq. 3 to experimental data. Mean ± SEM of two independent experiments

Results were fitted by Eq. 3 (*continuous trace*)

$$v = V_{\min} + \frac{V_{\max} - V_{\min}}{1 + \left(\frac{[\text{actin}]}{K_{D[\text{actin}]}}\right)^{n}}, \quad (3)$$

where "$V_{\max}$" and "$V_{\min}$" represent the PMCA activity in the absence of actin or when [actin] tends to infinity, respectively. $K_{D[\text{actin}]}$ corresponds to the F-actin concentration that produces half of Ca^{2+}-ATPase activity inhibition and, "n" is the Hill coefficient.

The parameter values obtained were $V_{\max} = 11.5 \pm 0.1$ μmol/(mg min), $V_{\min} = 6.2 \pm 0.1$ μmol/(mg min), $K_{D[\text{actin}]} = 0.68 \pm 0.02$ μM, and $n = 2 \pm 0.1$. The fact that submicromolar concentrations of actin only partially inhibit Ca^{2+}-ATPase activity suggests that this is a specific effect of the protein.

Effect of Actin on the PMCA Phosphoenzyme Levels

During the catalytic cycle, PMCA reacts with ATP to form acid-stable phosphorylated intermediates (EP) that can be measured using [γ^{32}P]ATP. Formation of the EP intermediate was identified and quantified using electrophoretic methods [19], by calculating the ratio of the EP levels from the autoradiogram and the total PMCA levels (E) from the Coomassie-stained SDS gel. Figure 4 shows the results of a typical experiment measuring the effects of G- and F-actin on EP levels (Fig. 4). Panel A shows an SDS-polyacrylamide gel of purified enzyme that was phosphorylated with 30 μM [γ^{32}P]ATP in the presence of 5 μM G-actin (lane E2), 5 μM F-actin (lane E3), or no actin (lane E1). Phosphorylation reactions were carried out for 1 min at 4 °C. Panel B shows the autoradiogram of the SDS-PAGE. The results from three independent experiments showed that G-actin and/or short oligomers increase the ratio of EP/E to 158.8 ± 6.4 %, while F-actin reduces this ratio to 49.7 ± 3.8 % with respect to the control. Therefore, these results suggest that according to its polymerization state, actin modifies the steady-state phosphorylation levels of the pump. This may constitute at least one of the possible mechanisms by which actin regulates the catalytic cycle of PMCA (i.e., by altering its turnover number).

Specific Incorporation of [^{125}I]TID-PC/16 on PMCA: Effect of G- and F-Actin on Conformation of PMCA Transmembrane Domain

We have described a simple technique that can identify changes in the accessibility to the phospholipid environment of PMCA [22]. By this strategy, we demonstrated that

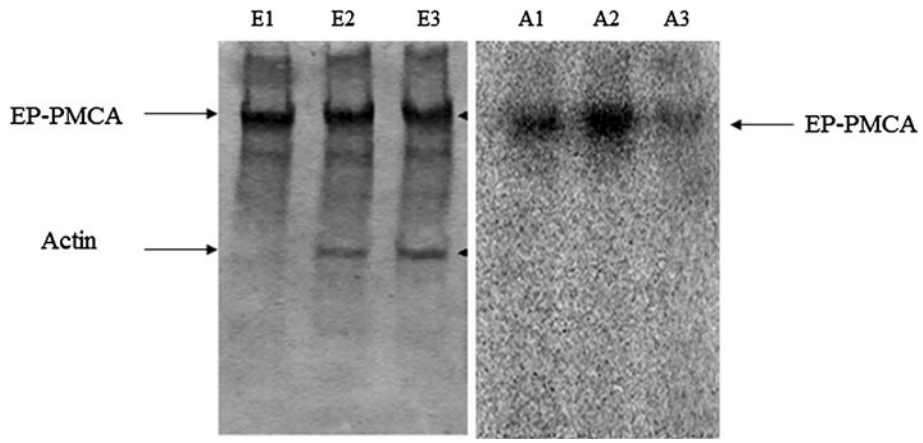

Fig. 4 Effect of actin on the phosphorylation of purified PMCA. *Left* SDS-PAGE. Phosphorylation was carried out as explained in "Experimental Procedures" section, incubating for 1 min in the absence (control *lane 1*) or in the presence of 5 μM G-actin (*lane E2*), or incubating in the presence of 5 μM G-actin for 18 min (*lane E3*). *Right* Autoradiogram. After electrophoresis, gels were stained with Coomassie Brilliant Blue R, dried, and exposed to an Image PhosphoScreen. The screen was scanned and the images were processed with ImageQuant to evaluate protein concentration. One representative experiment out of three independent experiments is shown (see text for quantification of results)

calmodulin activation involves a decrease in the accessible area to the lipids. This effect was observed for several treatments that produce activation of PMCA, such as removing the C-terminal autoinhibitory domain by controlled proteolysis, or addition of acidic phospholipids or unsaturated fatty acids, strongly suggesting that the process of pump activation involves to a conformational change in the transmembrane domain, whose distinguishing characteristic is associated with lower accessibility to lipid environment, i.e., a more compact conformation of the hydrophobic domain.

In order to assess whether the behavior of activation and inhibition observed in different states of actin polymerization could be related to a conformational changes in the PMCA transmembrane domain, we measured the specific incorporation of [^{125}I]TID-PC/16 to PMCA under conditions that promote the monomeric or polymeric form of actin. The incorporation of the probe to PMCA in the absence of calcium (in media with EGTA) was taken arbitrarily as 100 % (Fig. 5). As described previously [22], addition of Ca^{2+} shifts the conformational equilibrium toward the auto-inhibited E_1 form (E_1I), so that the specific incorporation is increased. When calmodulin is added in the presence of Ca^{2+} the equilibrium is displaced to the activated E_1 conformation (E_1A), and specific incorporation decreases by 50 %. The addition of actin in depolymerizing conditions (in the presence of Ca^{2+}) causes a decrease in the specific incorporation of [^{125}I]TID-PC/16, similar to that observed in the presence of calmodulin. Conversely, when F-actin was present, the specific incorporation of the probe was similar to that obtained in the presence of Ca^{2+} alone. These results suggest that activation of the PMCA ATPase activity observed in the presence of G-actin (or short oligomers) is associated with a conformational change in the transmembrane domain of the pump, a behavior similar to that observed with other treatments of activation [23].

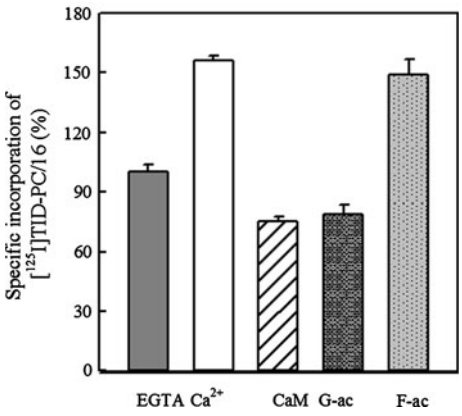

Fig. 5 Relative specific incorporation of [^{125}I]TID-PC/16 to PMCA was determined as described in "Experimental Procedures" section and in the presence of 1 mM EGTA (*EGTA*); 100 μM free Ca^{2+} (*Ca^{2+}*); 100 μM Ca^{2+} plus 200 nM calmodulin (*CaM*); 100 μM Ca^{2+} and 5 μM G-actin (*G-ac*) and 100 μM Ca^{2+} and 5 μM G-actin incubated 60 min in polymerizing medium before photolabelling of the sample (*F-ac*). Specific incorporation of the probe in the presence of EGTA was considered as 100 %. Mean ± SEM of three independent experiments

Binding of Actin to Purified PMCA

In order to determine whether the modulation of PMCA catalytic activity by actin is due to a direct interaction between these proteins, we tested the binding of actin to a purified and soluble preparation of PMCA using two different approaches:

(i) Aliquots of PMCA were spotted on a membrane and incubated with G- or F-actin (as described in "Experimental Procedures" section). After washing, the dot blots were developed using an actin antibody for detection. As controls, we tested PMCA in the absence of actin and BSA (instead of PMCA) incubated with actin. Figure 6 shows that anti-actin antibody detected both G- and F-actin in the presence of PMCA, whereas the controls (PMCA alone or BSA incubated with actin) were negative. As a further control, a sample was revealed with 5F10, a specific antibody for PMCA to confirm its presence. These results suggest that actin can bind to the enzyme in the conditions tested and rule out the possibility of non-specific cross-reaction of actin antibody with the PMCA.

(ii) We also tested the cosedimentation of F-actin with PMCA using an actin-binding spin-down assay kit based on the method described by Srivastava and Barber [20] for the quantification of protein binding

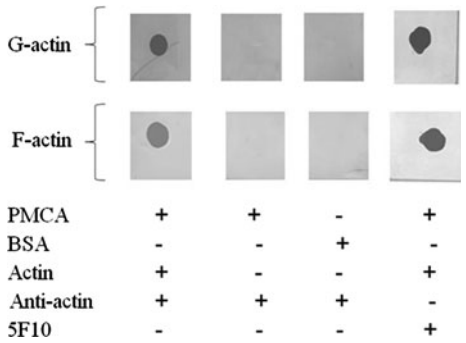

Fig. 6 Binding of actin to purified PMCA. Purified PMCA from human erythrocytes was blotted onto nitrocellulose membranes (see "Experimental Procedures" section) and revealed with anti-actin antibody in the presence of 5 μM monomeric actin or 5 μM actin which was allowed to polymerize. Controls were performed using BSA or no actin incubated under the same conditions. PMCA was also incubated in the absence of actin and visualized using 5F10 specific antibody as a control

to F-actin. The basic principle of this assay involves incubation of the protein of interest with F-actin followed by separation using sample centrifugation. F-actin-binding proteins will cosediment with actin filaments. The reaction medium was similar to that used for Ca^{2+}-ATPase activity measurements but without ATP and both proteins were incubated during 40 min before the ultracentrifugation. The amount of PMCA was 2 μg (about tenfold higher than for activity assays) due to the detection limit of the cosedimentation assay. The F-actin concentration was modified to maintain a constant ratio between both proteins.

Figure 7 shows a representative experiment in which samples of supernatant (Fig. 7a) and pellet (Fig. 7b) fractions obtained from cosedimentation assays were run in an SDS-PAGE. Lanes 1 and 2 show that PMCA buffer has no effect on F-actin sedimentation. α-actinin, a protein that binds F-actin and bundles it, was found in the supernatant in the absence of actin (lane 3), whereas 80 % was in the pellet in the presence of F-actin (lane 4). In contrast, 90 % of BSA remained in the supernatant even in the presence of actin (lanes 5 and 6). When PMCA was incubated with F-actin, both proteins were found in the pellet fraction (lane 8) but PMCA alone did not precipitate when actin was absent, i.e., PMCA was recovered in the supernatant fraction (lane 7). These results further suggest that F-actin interacts directly with PMCA.

In order to study the interaction between F-actin and PMCA using this approach, we performed a series of cosedimentation experiments like that described above but in the presence of different F-actin concentrations, and quantified the PMCA that was found in the pellet fraction. Figure 7c shows that the amount of PMCA sedimented increases in a saturable, sigmoidal way as a function of F-actin concentration (*closed circles*) while it concomitantly disappears from the supernatant (*open circles*). The binding of actin to PMCA shows a $K_{0.5}$ of 8.4 μM. In agreement with the experiment of Ca^{2+}-ATPase activity, the cosedimentation assay confirms a direct interaction between F-actin and PMCA.

Discussion

We have previously reported that the specific activity of the Ca^{2+}-ATPase in erythrocyte membranes has an unexpected dependence on the membrane protein concentration [1]. The experiments in the current study were designed to test the hypothesis that this phenomenon of activation–inhibition of the specific activity of PMCA is linked to the actin cytoskeleton present in the preparation. Results in this paper suggest that the effect of membrane protein dilution on specific PMCA activity is related to the concentration of actin, which is reduced in IOVs. This phenomenon may be related to the depolymerization of actin [25, 26] because purified PMCA from red blood cell membranes and

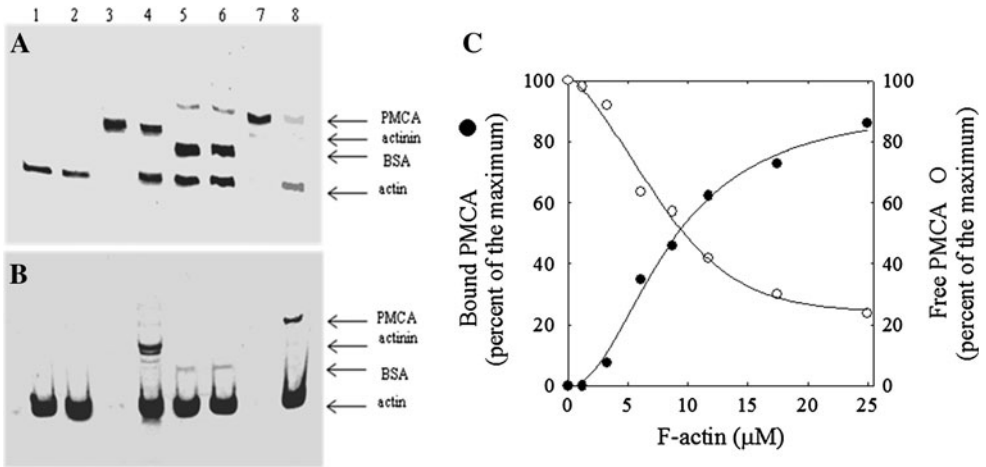

Fig. 7 Cosedimentation of actin and PMCA. **a** Proteins in the supernatants and **b** proteins in the pellets. The content of lanes is as follows: (*1*) actin incubated in the buffer used to suspend PMCA, (*2*) actin suspended in the reaction buffer, (*3*) α-actinin, (*4*) α-actinin incubated with actin, (*5*) BSA in the presence of actin, (*6*) BSA previously centrifuged at 100,000×*g* and then incubated with actin, (*7*) PMCA, and (*8*) PMCA incubated with actin. The concentrations of actin and PMCA were 17.5 μM and 15 nM, respectively. **c** Concentration of PMCA in the pellet (*filled circle* bound PMCA) and supernatant (*open circle* free PMCA) as a function of G-actin concentration previously polymerized. PMCA was brought into contact with clarified actin and incubated under conditions which promote the polymerization for 40 min. The samples were spun down for 20 min at 100,000×*g*. The proteins present in the supernatants were precipitated with TCA 10 % and the pellet separated by SDS-PAGE. After staining with Coomassie Blue, bands were quantified as described in "Experimental Procedures" section

presumably, any purified PMCA reconstituted in a pure lipid membrane, does not display any dependence of its specific activity on dilution [1].

To further test this hypothesis, we measured the effect of actin on purified PMCA under conditions in which the polymerization process was favored (Fig. 2). As expected, in the first stages of polymerization, PMCA specific activity was higher than that of the control where BSA was replacing actin. Moreover, this activation decreases as the actin polymerization progresses to reach a constant value. In this new steady state of the system, actin remains in the filamentous form and the activity of the pump is lower than that of the control. The fact that the change in activity ($k = 0.6$ min^{-1}) is reached somewhat earlier than the completion of polymerization ($k = 0.17$ min^{-1}) could indicate that loss of activation involves disappearance of monomers and short oligomers, while inhibition by polymerized actin would start before full-length filaments are formed.

To study the effect of F-actin on PMCA, we measured the Ca^{2+}-ATPase activity of the pump in the presence of different concentrations of G-actin under polymerizing conditions (Fig. 3). Actin causes an increase in the medium viscosity when polymerized [27], which could be the reason of the decrease in pump activity [28]. However, while Ca^{2+}-ATPase activity decreases toward zero with increasing glycerol concentrations (data not shown), it is only partially inhibited by submicromolar–micromolar concentrations of actin (Fig. 3), which suggests a specific effect of the protein on PMCA. This hypothesis is not opposed to the idea of a mechanism involving changes of viscosity in the microenvironment of the enzyme [28]. In experiments using media that promote actin polymerization, Vanagas et al. [1] showed that the half-maximal concentrations of ATP and calmodulin for activation of the pump are not affected by total protein concentration, concluding that accessibility of the substrates would not be the cause of the decreased Ca^{2+}-ATPase activity observed.

When investigating the effects of glycerol and polyethylene glycol on the sodium pump functioning, Esmann et al. [28] proposed that overall enzymatic activities of this transport ATPase are associated with large changes in hydration volumes involving several hundreds of water molecules. These are probably buried within the protein, and a possible candidate is a large cluster of water molecules near the phosphorylation site that could be displaced by glycerol. In agreement, our results show that actin differentially affects the steady-state levels of PMCA-phosphorylated intermediates. Furthermore, the EP level was well correlated to the observed effect on the Ca^{2+}-ATPase activity.

In the presence of calcium, G-actin decreases the specific incorporation of [^{125}I]TID-PC/16; however, F-actin does not produce any detectable change (Fig. 5). A difference in the area accessible to lipids can only occur as consequence of the existence of two different conformations of the pump. The opposite is not necessarily true, however, a similar value of specific incorporation of [^{125}I]TID-PC/16 does not necessarily reflect similar conformations, as different arrangements of the transmembrane helices could yield the same values of total surface accessible to lipids. Thus, our results suggest that G-actin (or short oligomers of it) leads to a more compact conformation of the transmembrane domain, while the inhibition by F-actin does not involve changes in the accessible lipid area of the transmembrane domain.

Results from immunoblotting and cosedimentation experiments suggest the presence of a direct interaction between the purified proteins. The sigmoidicity of the results in Fig. 7c is difficult to interpret, as the length of filaments depends on the concentration of actin [29] and a minimal average length could be necessary to insure the cosedimentation of the complex with PMCA. This also could explain the low apparent affinity of the phenomenon as compared to that observed for the results of ATPase activity in Fig. 3.

Diffusion within the fluid membrane plays an important role for cellular processes, because the cell communicates with its surroundings via its lipid bilayer [30]. The dynamics of interactions in the membrane skeleton control a variety of critical red cell membrane properties. Actin-binding proteins can sever, cap, nucleate, or bundle actin filaments or sequester monomeric G-actin, thus altering the gel–sol state of the cortical structure, and initiate changes in the cortical cytoskeleton [2]. In particular, sensitive parameters are deformability under prolonged shear and glycoprotein lateral diffusion rates [30, 31]. Auth et al. [30] propose a new model for the steric hindrance of protein diffusion in the cell membrane that is directly related to the local density of flexible cytoskeletal filaments anchored to the membrane and to the protein size. Their model goes beyond simple corral models, as it describes barrier heights and widths based on the physical properties of the cytoskeletal filaments.

Alterations in membrane fluidity accompanied by changes in the actin membrane cytoskeleton have been demonstrated to increase Na^+,K^+-ATPase activity in the basolateral membrane of epithelial cells [32]. Changes in ion transport require spatially and temporally coordinated changes in cell morphology and cell motility, and these changes can be brought about by changes in actin dynamics [2]. There is a great difference between the membrane system and a system in which both proteins are isolated; therefore, we evaluated the effect of F-actin on PMCA activity under the same conditions performed in cosedimentation experiments (Fig. 3). The apparent inhibitory constant for F-actin effect on PMCA (K_i) was 0.68 ± 0.02 μM. This value was significantly higher than the one obtained in membranes or IOVs preparations (see Fig. 1).

Referring to the cosedimentation assays, it is not permissible to compare the values of the inhibitory constant and the binding constant because of the great difference between the experimental conditions and the preparations used, especially considering the possibility that not all the complex with PMCA is detectable by the cosedimentation assay at low concentrations of actin. The data show that actin can interact directly with PMCA in vitro. These data do not, however, rule out the possibility that interactions with other components of the actin cytoskeleton regulate PMCA activity in the cell.

Padanyi et al. [33] reported that the lateral membrane mobility of the clustered PMCA4b is significantly lower than that of the non-clustered molecules; they suggest that PSD-95 promotes the formation of high-density PMCA4b microdomains in the plasma membrane and that the membrane cytoskeleton plays an important role in the regulation of this process. Moreover, they recently suggested that the actin filaments under the plasma membrane play an essential although different role in the scaffolding of specific PMCA isoforms, where NHERF2 anchors PMCA2w/b to the apical actin filaments via ezrin. Thus, the interaction with specific scaffolding proteins can assemble the different PMCA isoforms into distinct structured units that are stabilized (either fenced or anchored) by the actin cytoskeleton [34].

PMCA pumps interact with numerous proteins. Some interacting partners are involved in the recruitment and maintenance of particular PMCA isoforms in specific membrane domains; others regulate the pump's ability to export Ca^{2+} from cells [35]. For example, PMCA, alpha-1 syntrophin, and NOS-1 have been found to form a ternary complex in cardiac myocytes [36]. Syntrophins are also linked to the actin cytoskeleton, supporting the notion that PMCAs are connected to the underlying membrane cytoskeleton. In 1995, Cantiello [5] reported that the Na^+- and K^+-dependent, ouabain-sensitive ATP hydrolysis mediated by rat kidney Na^+,K^+-ATPase increased by 74 % in the presence of previously non-polymerized actin, whereas addition of polymerized actin was without effect. In red blood cell membranes, we found a similar effect of membrane dilution on the Na^+/K^+ pump as for PMCA (unpublished observations), indicating that at least for cell membranes containing low pump density, actin may activate or inhibit the sodium pump depending on its state of polymerization. Thus, the actin-dependent activation–inhibition effect may be a more general property of membrane proteins in which the cytoskeleton is no longer restricted providing a mechanical function, but rather participates directly in the modulation of the activity of integral proteins to which it is attached.

Our study provides evidences for a direct, dynamic interaction between PMCA and the actin cytoskeleton. Additional experiments are in course in order to identify the underlying regulatory mechanism and the PMCA specific domains which actin may interact with.

Acknowledgments The present work was supported by the NIH, Fogarty International Center Grant R03TW006837 to JPFCR and by ANPCYT, CONICET and UBACYT from Argentina. MCDLF, LV, MD, and MFG are doctoral fellows of CONICET. ICM, RCR and JPFCR are established investigators of CONICET, Argentina. EES is an established researcher of Mayo/Clinic Foundation, Rochester, MN, USA.

References

1. Vanagas, L., Rossi, R. C., Caride, A. J., Filoteo, A. G., Strehler, E. E., & Rossi, J. P. (2007). Plasma membrane calcium pump activity is affected by the membrane protein concentration: Evidence for the involvement of the actin cytoskeleton. *Biochimica et Biophysica Acta, 1768*, 1641–1644.
2. Khurana, S. (2000). Role of actin cytoskeleton in regulation of ion transport: Examples from epithelial cells. *Journal of Membrane Biology, 178*, 73–87. (Review).
3. Cooke, R. (1975). The role of the bound nucleotide in the polymerization of actin. *Biochemistry, 14*, 3250–3256.
4. Bertorello, A. M., Ridge, K. M., Chibalin, A. V., Katz, A. I., & Sznajder, J. I. (1999). Isoproterenol increases Na^+–K^+-ATPase activity by membrane insertion of alpha-subunits in lung alveolar cells. *American Journal of Physiology, 276*, L20–L27.
5. Cantiello, H. F. (1995). Actin filaments stimulate the Na(+)–K(+)-ATPase. *American Journal of Physiology, 1995*(269), F637–F643.
6. González Flecha, F. L., Castello, P. R., Caride, A. J., Gagliardino, J. J., & Rossi, J. P. (1993). The erythrocyte calcium pump is inhibited by non-enzymic glycation: Studies in situ and with the purified enzyme. *Biochemical Journal, 1993*(293), 369–375.
7. Steck, T. L., Weinstein, R. S., Straus, J. H., & Wallach, D. F. (1970). Inside-out red cell membrane vesicles: Preparation and purification. *Science, 168*, 255–257.
8. Ellman, G. L., Courtney, K. D., Andres, V, Jr, & Feather-Stone, R. M. (1961). A new and rapid colorimetric determination of acetylcholinesterase activity. *Biochemical Pharmacology, 7*, 88–95.
9. Filomatori, C. V., & Rega, A. F. (2003). On the mechanism of activation of the plasma membrane Ca^{2+}-ATPase by ATP and acidic phospholipids. *Journal of Biological Chemistry, 278*, 22265–22271.
10. Pardee, J. D., & Spudich, J. A. (1982). Purification of muscle actin. *Methods in Enzymology, 85*(Pt B), 164–181.
11. Xu, S., Malinchik, S., Frisbie, S., Gu, J., Kraft, T., Rapp, G., et al. (1998). X-ray diffraction studies of the cross-bridge intermediate states. *Advances in Experimental Medicine and Biology, 453*, 271–278. discussion 278–279.
12. Cooper, J. A., Walker, S. B., & Pollard, T. D. (1983). Pyrene actin: Documentation of the validity of a sensitive assay for actin polymerization. *Journal of Muscle Research and Cell Motility, 4*, 253–262.
13. Webb, M. R. (1992). A continuous spectrophotometric assay for inorganic phosphate and for measuring phosphate release kinetics in biological systems. *Proceedings of the National Academy of Sciences of the United States of America, 89*, 4884–4887.
14. Fiske, C. H., & Subbarrow, Y. (1925). The colorimetric determination of phosphorus. *Journal of Biological Chemistry, 66*, 375–400.
15. Schaegger, H., & Von Jagow, (1987). Tricine-sodium dodecyl sulfate polyacrylamide gel electrophoresis for the separation of

proteins in the range from 1 to 100 kDa. *Analytical Biochemistry, 166*, 368–379.
16. Lündahl, P. (1975). Proteins selectively released from water-extracted human erythrocyte membranes upon citranylation or maleylation. *Biochimica et Biophysica Acta, 379*, 304–316.
17. Peterson, G. L. (1983). Determination of total protein. *Methods in Enzymology, 91*, 95–121.
18. Ball, E. H. (1986). Quantitation of proteins by elution of coomassie brilliant blue R from stained bands after sodium dodecyl sulfate-polyacrylamide gel electrophoresis. *Analytical Biochemistry, 1986*(155), 26–27.
19. Echarte, M. M., Levi, V., Villamil, A. M., Rossi, R. C., & Rossi, J. P. (2001). Quantitation of plasma membrane calcium pump phosphorylated intermediates by electrophoresis. *Analytical Biochemistry, 289*, 267–273.
20. Srivastava, J., & Barber, D. (2008). Actin co-sedimentation assay for the analysis of protein binding to F-actin. *Journal of Visualized Experiments, 28*, 690.
21. Weber, T., & Brunner, J. (1995). Photolabeling identifies a putative fusion domain in the envelope glycoprotein of rabies and vesicular stomatitis viruses. *Journal of the American Chemical Society, 117*, 3084–3095.
22. Mangialavori, I., Giraldo, A. M., Buslje, C. M., Gomes, M. F., Caride, A. J., & Rossi, J. P. (2009). A new conformation in sarcoplasmic reticulum calcium pump and plasma membrane Ca^{2+} pumps revealed by a photoactivatable phospholipidic probe. *Journal of Biological Chemistry, 284*, 4823–4828.
23. Mangialavori, I., Ferreira-Gomes, M. F., Pignataro, M. F., Strehler, E. E., & Rossi, J. P. (2010). Determination of the dissociation constants for Ca^{2+} and calmodulin from the plasma membrane Ca^{2+} pump by a lipid probe that senses membrane domain changes. *Journal of Biological Chemistry, 285*, 123–130.
24. Dzandu, J. K., Deh, M. E., Barratt, D. L., & Wise, G. E. (1981). Detection of erythrocyte membrane proteins, sialoglycoproteins, and lipids in the same polyacrylamide gel using a double-staining technique. *Proceedings of the National Academy of Sciences of the United States of America, 81*, 1733–1737.
25. Purich, D. L., & Southwick, F. S. (1999). Energetics of nucleotide hydrolysis in polymer assembly/disassembly: The cases of actin and tubulin. *Methods in Enzymology, 308*, 93–111.
26. Karr, T. L., & Kristofferson, D. (1980). Mechanism of microtubule depolymerization. Correlation of rapid induced disassembly experiments with a kinetic model for endwise depolymerization. *Journal of Biological Chemistry, 255*, 8560–8566.
27. Scott, K. Z., & Stossel, T. P. (1983). Physical basis of the rheologic properties of F-actin. *Journal of Biological Chemistry, 25*, 11004–11009.
28. Esmann, M., Fedosova, N. U., & Marsh, D. (2008). Osmotic stress and viscous retardation of the Na,K-ATPase ion pump. *Biophysical Journal, 95*, 2767–2776.
29. Käs, J., Strey, H., Tang, J. X., Finger, D., Ezzell, R., Sackmann, E., et al. (1996). F-actin, a model polymer for semiflexible chains in dilute, semidilute, and liquid crystalline solutions. *Biophysical Journal, 70*, 609–625.
30. Auth, T., & Gov, N. S. (2009). Diffusion in a fluid membrane with a flexible cortical cytoskeleton. *Biophysical Journal, 96*, 818–830.
31. Sheetz, M. P. (1983). Membrane skeletal dynamics: Role in modulation of red cell deformability, mobility of transmembrane proteins, and shape. *Seminars in Hematology, 20*, 175–188.
32. Molitoris, B. A., Dahl, R., & Geerdes, A. (1992). Cytoskeleton disruption and apical redistribution of proximal tubule Na(+)–K(+)-ATPase during ischemia. *American Journal of Physiology, 263*, 488–495.
33. Padanyi, R., Paszty, K., Strehler, E. E., & Enyedi, A. (2009). PSD-95 mediates membrane clustering of the human plasma membrane Ca^{2+} pump isoform 4b. *Biochimica et Biophysica Acta, 1793*, 1023–1032.
34. Padanyi, R., Xiong, Y., Antalffy, G., Lor, K., Paszty, K., Strehler, E. E., et al. (2010). Apical scaffolding protein NHERF2 modulates the localization of alternatively spliced plasma membrane Ca^{2+}– Pump 2B variants in polarized epithelial cells. *Journal of Biological Chemistry, 285*, 1704–31712.
35. Akiyama, T., Kadowaki, T., Nishida, E., Kadooka, T., Ogawara, H., Fukami, Y., et al. (1986). Substrate specificities of tyrosine-specific protein kinases toward cytoskeletal proteins in vitro. *Journal of Biological Chemistry, 261*, 14797–14803.
36. Agnew, B. J., Duman, J. G., Watson, C. L., Coling, D. E., & Forte, J. G. (1999). Cytological transformations associated with parietal cell stimulation: Critical steps in the activation cascade. *Journal of Cell Science, 112*, 2639–2646.